

Synthesis and Characterization of Trigonal Gold(I) Cage Complexes: Luminescent Metallocryptates Encapsulating Tl(I) and Na⁺ Ions

Vincent J. Catalano,* Byron L. Bennett, and Heidi M. Kar

Department of Chemistry, University of Nevada
Reno, Nevada 89557

Bruce C. Noll

Department of Chemistry and Biochemistry
University of Colorado, Boulder Colorado 80309

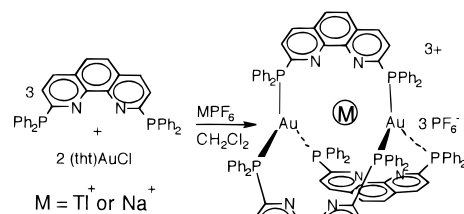
Received June 14, 1999

The aurophilicity principle is often used to describe the strong, closed-shell metal–metal interactions of gold compounds.¹ There are numerous examples of linear, two-coordinate Au(I) complexes associating with themselves or other closed-shell ions such as Tl(I) or Pb(II) producing aggregates with intermetallic separations shorter than the sum of the van der Waals radii.² Many of these complexes form highly luminescent, extended arrays in the solid state; however, upon dissolution these assemblages tend to dissociate into their nonemissive, monomeric components.^{1d,2a,b} Synthetic manipulation of the ligand backbone provides a mechanism for inducing a solution-state interaction by providing auxiliary donor sites for ion binding, and a fair number of late transition metal Tl(I) and Pb(II) interactions have been probed.³ Surprisingly, the interactions between highly luminescent, trigonal Au(I) centers and Tl(I) have not been probed. Here we report a novel host complex based on trigonal Au(I) centers, its complexation of Tl(I) ion and Na⁺ ions, and its luminescent properties.

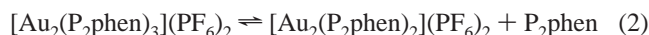
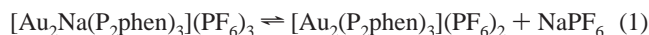
The gold-based metallocryptates were synthesized according to Scheme 1. A dichloromethane solution of 2,9-bis(diphenylphosphino)-1,10-phenanthroline (P₂-phen) ligand⁴ was treated with 1 equiv of MPF₆ (M = Tl or Na) followed by 2/3 equiv of Au-(tht)Cl (tht is tetrahydrothiophene) affording the pale-yellow [Au₂-Tl(P₂-phen)₃](PF₆)₃, **1**, or yellow [Au₂Na(P₂-phen)₃](PF₆)₃, **2**, respectively. The ³¹P{¹H} NMR spectra of **1** (acetone-*d*₆/MeOH) shows a resonance at 45.7 ppm while **2** (CDCl₃/CH₂Cl₂) shows a singlet at 45.5 ppm. Additionally, the spectrum of **1** displays coupling to ²⁰⁵Tl (d, ²J_{Tl-P} = 186 Hz). This assignment is confirmed by the observation of a septet (δ 749.9 ppm, ²J_{P-Tl} = 186 Hz) in the ²⁰⁵Tl NMR spectrum⁵ indicating a single ²⁰⁵Tl environment coupled to six chemically equivalent P atoms.

Unlike complex **1**, the ³¹P{¹H} NMR spectrum of **2** indicates that [Au₂Na(P₂-phen)₃](PF₆)₃ is dynamic. In a fast exchange mechanism a chlorocarbon solution of **2** loses a Na⁺ ion and dissociates a P₂phen ligand producing an equilibrium mixture of the empty metallocryptand, [Au₂(P₂-phen)₃](PF₆)₂, a two-coordinate, gold macrocycle,⁶ [Au₂(P₂-phen)₂](PF₆)₂, free ligand, NaPF₆, and **2** according to eqs 1 and 2. The equilibrium constant for eq 1 is measured to be ~5 with [Au₂(P₂-phen)₃](PF₆)₂ as the dominant

Scheme 1



species. For eq 2 the empty metallocryptand is favored ($K \approx 1.6 \times 10^{-4}$). Addition of TlNO₃ to this equilibrium mixture produces **1** exclusively.



X-ray diffraction studies⁷ support the formulation of **1** and **2**. Views of the cations are presented in Figures 1 and 2. Both structures contain two trigonal Au(I) centers capping a *D*₃ symmetric cage. In **1** the gold centers strongly interact with the Tl(I) ion with Au(1)–Tl(1) and Au(2)–Tl(1) separations of 2.9171(5) and 2.9109(5) Å, whereas in **2**, the Na⁺ ion is more loosely held. Its position is effectively modeled in three partially occupied sites, each one slightly off center and canted toward a phenanthroline ring. The average of the Au–Na–Au angles is 163.4°. In **1** the Tl–N distances (av 3.23 Å) are long indicating that the Au–Tl interactions are the predominant attractive forces holding the Tl(I) ion in this cage. In contrast, the encapsulated Na⁺ ion is expected to have a repulsive interaction with the gold centers, and it is likely that the phenanthroline bases are responsible for maintaining this assembly. For comparison, the average Na–N distances observed in Lehn's Na(phenanthroline)₃ and Na(tris(bipyridine)cryptate) complexes are significantly shorter at 2.780 and 2.79 Å, respectively, indicating that the cavities formed by **1** and **2** are much larger.⁸ The strong Au–Tl interactions in **1** are further manifested in the deviations in planarity of the AuP₃ units. In **1** the Au(1) and Au(2) atoms are displaced outward by 0.125 and 0.167 Å from their respective phosphine planes while in **2** the deviations are larger at 0.230 and 0.237 Å, respectively. However, the intramolecular Au(1)···Au(2) separations show the opposite trend at 5.821 Å

(6) [Au₂(P₂-phen)₂](PF₆)₂ was characterized by X-ray crystallography (Supporting Information) and NMR spectroscopy (³¹P{¹H} NMR δ 45.5 ppm, CDCl₃).

(7) A yellow crystal of **1** obtained by slow diffusion of benzene into a 1,2-dichloroethane solution of [Au₂Tl(P₂-phen)₃](ClO₄)₃ was mounted into the –135 °C nitrogen cold stream of a Siemens SMART diffractometer equipped with a CCD detection system with graphite monochromated Mo Kα radiation. Crystal data for [Au₂Tl(P₂-phen)₃](ClO₄)₃·1,2-Cl₂(CH₂)₂·3C₆H₆: monoclinic space group, *P*2₁/*n*, *a* = 18.176(4) Å, *b* = 24.249(5) Å, *c* = 26.356(5) Å, β = 101.01(4)°, *V* = 11403.3(7) Å³, *Z* = 4. A total of 84 672 reflections were measured and 26 165 unique reflections (2θ < 55°, *R*_{int} = 0.131) were used in the refinement. Full-matrix least-squares refinement on *F*² converged to *R*_F = 0.1594 (all data), 0.0671 (*I* > 2σ(*I*)); *R*_{wF²} = 0.1345 (all data), 0.1123 (*I* > 2σ(*I*)). Hydrogen atoms were added using a riding model with thermal parameters 1.2 times that of the host atom. An orange block of **2** obtained by slow diffusion of benzene into a 1,2-dichloroethane solution of [Au₂Na(P₂-phen)₃](PF₆)₃ was treated analogously to **1**. Crystal data for [Au₂Na(P₂-phen)₃](PF₆)₃·1,2-Cl₂(CH₂)₂·C₆H₆: monoclinic space group, *P*2₁/*n*, *a* = 18.404(4) Å, *b* = 24.336(5) Å, *c* = 27.089(5) Å, β = 101.39(5)°, *V* = 11893(2) Å³, *Z* = 4. A total of 88 725 reflections were measured and 27 280 unique reflections (2θ < 55°, *R*_{int} = 0.0625) were used in the refinement. Full-matrix least-squares refinement on *F*² converged to *R*_F = 0.0974 (all data), 0.0547 (*I* > 2σ(*I*)); *R*_{wF²} = 0.1520 (all data), 0.1349 (*I* > 2σ(*I*)).

(8) (a) Echegoyen, L.; DeCain, A.; Fischer, J.; Lehn, J.-M. *Angew. Chem., Int. Ed. Engl.* **1991**, *30*, 838–840. (b) Caron, A.; Guilhem, J.; Riche, C.; Pascard, C.; Alpha, B.; Lehn, J.-M.; Rodrigues-Ubis, C. *Helv. Chim. Acta* **1985**, *68*, 1577–1582.

(1) (a) Pyykkö, P.; Mendizabal, F. *Inorg. Chem.* **1998**, *37*, 3018. (b) Pyykkö, P. *Chem. Rev.* **1997**, *97*, 597. (c) Assefa, Z.; DeStefano, F.; Garepapaghi, M. A.; LaCasce, J. H., Jr.; Ouellete, S.; Corson, M. R.; Nagle, J. K.; Patterson, H. H. *Inorg. Chem.* **1991**, *30*, 2868. (d) Che, C.-M.; Wong, W.-T.; Lai, T.-F.; Kwong, H.-L. *J. Chem. Soc., Chem. Commun.* **1989**, 243–244. (e) King, C.; Wang, J.-C.; Khan, M. N. I.; Fackler, J. P., Jr. *Inorg. Chem.* **1989**, *28*, 2145–2149. (f) Schmidbaur, H. *Chem. Soc. Rev.* **1995**, 391.

(2) (a) Crespo, O.; Fernandez, E. J.; Jones, P. G.; Laguna, A.; Lopez-de-Luzuriaga, J. M.; Mendia, A.; Monge, M.; Olmos, E. *J. Chem. Soc., Chem. Commun.* **1998**, 2233. (b) Wang, S.; Garzón, G.; King, C.; Wang, J.-C.; Fackler, J. P., Jr. *Inorg. Chem.* **1989**, *28*, 4623.

(3) (a) Balch, A. L.; Neve, F.; Olmstead, M. M. *J. Am. Chem. Soc.* **1991**, *113*, 2995. (b) Balch, A. L.; Nagle, J. K.; Olmstead, M. M.; Reedy, P. E., Jr. *J. Am. Chem. Soc.* **1987**, *109*, 4124. (c) Casado, M. A.; Pérez-Torrente, J.; López, J. A.; Ciriano, M. A.; Lahoz, F. J.; Oro, L. A. *Inorg. Chem.* **1999**, *38*, 2482.

(4) Ziessel, R. *Tetrahedron Lett.* **1989**, *30*, 463.

(5) ²⁰⁵Tl NMR spectra (288.537 MHz) were referenced vs TlNO₃(aq).

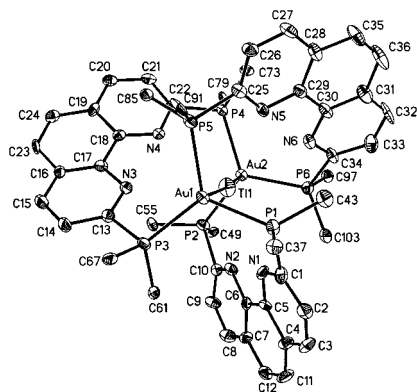


Figure 1. Thermal ellipsoid plot (50% probability) of the cation of $[\text{Au}_2\text{-Tl}(\text{P}_2\text{Phen})_3](\text{ClO}_4)_3$, **1**, with phenyl rings and hydrogen atoms omitted for clarity. Selected bond lengths (Å) and angles (deg) for **1**: Au(1)–Tl(1) 2.9171(5), Au(2)–Tl(1) 2.9109(5), Tl(1)–N(1) 3.178(5), Tl(1)–N(2) 3.208(5), Tl(1)–N(3) 3.321(5), Tl(1)–N(4) 3.193(5), Tl(1)–N(5) 3.329(5), Tl(1)–N(6) 3.158(5), Au(1)–P(1) 2.388(3), Au(1)–P(3) 2.381(2), Au(1)–P(5) 2.380(2), Au(2)–P(2) 2.368(2), Au(2)–P(4) 2.377(2), Au(2)–P(6) 2.381(3), Au(1)–Tl(1)–Au(2) 174.47(2).

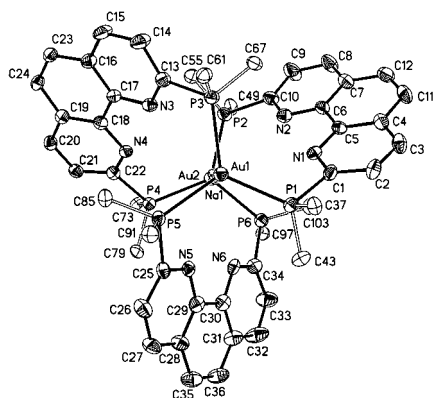


Figure 2. Thermal ellipsoid plot (50% probability) of the cation of $[\text{Au}_2\text{-Na}(\text{P}_2\text{Phen})_3](\text{PF}_6)_3$, **2**, with hydrogen atoms and phenyl rings omitted for clarity. Only one position of the Na ion is shown. Selected bond lengths (Å) and angles (deg) for **2**: Au(1)–Na(1) 2.797(13), Au(2)–Na(1) 2.813(13), Na(1)–N(1) 3.471(7), Na(1)–N(2) 3.427(7), Na(1)–N(3) 3.260(7), Na(1)–N(4) 3.294(7), Na(1)–N(5) 3.343(7), Na(1)–N(6) 3.368(7), Au(1)–P(1) 2.3701(16), Au(1)–P(3) 2.3685(16), Au(1)–P(5) 2.3662(15), Au(2)–P(2) 2.3615(16), Au(2)–P(4) 2.3627(16), Au(2)–P(6) 2.3716(17), Au(1)–Na(1)–Au(2) 177.4(6), Au(1)–Na(1A)–Au(2) 155.7(2), Au(1)–Na(1)–Au(2) 157.2(5).

for **1** and 5.609 Å for **2**. These separations are consistent with the observation of the smaller average P–Au–Au–P torsion angles for **2** (104°) compared to **1** (109°). Both **1** and **2** are helical with a 3-fold rotational axis about each Au(I) atom; however, as dictated by the centrosymmetric space group they are racemic.

The electronic absorption spectra of **1** and **2** exhibit strong $\pi\text{-}\pi^*$ bands between 250 and 300 nm. Additionally, **1** shows a weak band at 402 nm ($\epsilon = 1800 \text{ M}^{-1} \text{ cm}^{-1}$) which, based on the excitation spectrum (Figure 3), may be a metal-centered triplet state. The corresponding singlet state is buried beneath a shoulder at 313 nm ($\epsilon = 40000 \text{ M}^{-1} \text{ cm}^{-1}$). This shoulder is also present in the free ligand and can be assigned to a ligand-centered band. Excitation of **1** (CH_3CN) at 340 or 420 nm results in an intense emission at 600 nm (Figure 3). The same behavior is observed in methanol, DMSO, or chlorocarbon solvent and in the solid state. This red emission can be assigned to a metal-centered phosphorescence process based on its large Stoke's shift, long solution-state lifetime (10 μs), long rise time (90 ns), and solvent independence.⁹ In the solid state this lifetime increases to 220 μs . Based on the short lifetime (<10 ns) the high energy feature at 390 nm is likely a fluorescence process.

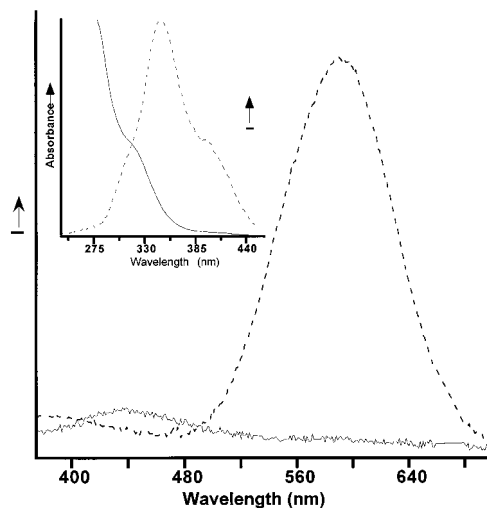


Figure 3. Emission spectra of **1** (dashed line) and of **2** (solid line) in acetonitrile with $\lambda_{\text{exi}} = 340 \text{ nm}$. Inset: Electronic absorption (solid line) and excitation (dashed line, $\lambda_{\text{mon}} = 590 \text{ nm}$) spectra of **1** (CH_3CN).

By comparison the corresponding Na^+ species, **2**, is considerably less emissive in the fluid state. The emission spectrum of the equilibrium mixture of **2** ($\lambda_{\text{exi}} = 340 \text{ nm}$, CH_3CN) exhibits a weak band at 440 nm along with a much less intense band at 580 nm. In the absence of sodium ion, the equilibrium mixture (eq 2) shows only a very weak emission at 535 nm (CH_3CN , $\lambda_{\text{exi}} = 340$) consistent with a trigonal AuP_3 center¹⁰ and a moderate signal at 440 nm, indicating that the 580 nm emission observed for **2** likely originates from small amounts of $[\text{Au}_2\text{Na}(\text{P}_2\text{phen})_3](\text{PF}_6)_3$ present in solution. Neither the P_2Phen ligand nor the macrocycle byproduct emit at 580 nm. The 440 nm band appears in all of these species including the free ligand and is likely a ligand-centered fluorescence process.

The nature of the intense emission from **1** can be attributed to the strong Au–Tl interaction. Although formally nonbonding, the trigonal Au centers have a strong affinity for Tl(I) ion. A qualitative MO diagram, similar to that proposed by Balch and co-workers,^{3b} can be constructed using filled Au $5d_z^2$, empty Au $6p_z$, Tl $6s$, and Tl $6p_z$ orbitals. Mixing between levels stabilizes the filled orbitals relative to their unfilled counterparts leading to an attractive interaction between these metals. Further, Fackler and co-workers^{3b} have employed a similar model with additional relativistic contributions from the Au $6s$ orbital to describe attractive Au–Tl interactions.

The metallocryptate methodology employed here offers a relatively simple strategy for producing a variety of $\text{AuP}_3\text{-M}'$ interactions, and to our knowledge **1** is the first reported trigonal $\text{AuP}_3\text{-Tl}$ interaction. Other d^{10} ions (Pt(0) or Pd(0)) readily form cryptates analogous to **1**, and we are currently exploring their chemical and physical properties.

Acknowledgment is made to the National Science Foundation for their generous financial support (CHE-9624281), to Prof. Michael G. Hill and Randy Villahermosa for assistance with measuring the emission lifetimes, and to Mr. Lewis Cary for assistance with the ^{205}Tl NMR spectroscopy.

Supporting Information Available: Tables of complete experimental and crystal structure data for **1**, **2**, and $[\text{Au}_2(\text{P}_2\text{phen})_2](\text{PF}_6)_2$ (PDF). This material is available free of charge via the Internet at <http://pubs.acs.org>.

JA991982E

(9) (a) Forward, J. M.; Fackler, J. P., Jr.; Assefa, Z. In *Optoelectronic Properties of Inorganic Compounds*; Roundhill, D. M., Fackler, J. P., Jr., Eds.; Plenum Press: New York, 1999; pp 195–226. (b) McCleskey, T. M.; Gray, H. B. *Inorg. Chem.* **1992**, *31*, 1733. (c) Jaw, H.-R. C.; Savas, M.; Mason, W. R. *Inorg. Chem.* **1989**, *28*, 4366.

(10) Fackler, J. P., Jr.; Grant, T. A.; Hanson, B. E.; Staples, R. J. *Gold Bull.* **1999**, *32*, 20.